# Repairable Modular Structural-Architectural Shear Walls

Mohammad Syed<sup>1</sup>; Grace F. Crocker<sup>2</sup>; Negar Elhami-Khorasani<sup>3</sup>; Pinar Okumus<sup>4</sup>; Brandon E. Ross<sup>5</sup>; and Michael Carlos Barrios Kleiss<sup>6</sup>

<sup>1</sup>Graduate Research Assistant, Dept. of Civil, Structural, and Environmental Engineering, Univ. at Buffalo, Buffalo, NY (corresponding author). Email: s54@buffalo.edu

<sup>2</sup>Graduate Research Assistant, Glenn Dept. of Civil Engineering, Clemson Univ., Clemson, SC. Email: gfulmer@g.clemson.edu

<sup>3</sup>Assistant Professor, Dept. of Civil, Structural, and Environmental Engineering, Univ. at Buffalo, Buffalo, NY. Email: negarkho@buffalo.edu

<sup>4</sup>Associate Professor, Dept. of Civil, Structural, and Environmental Engineering, Univ. at Buffalo, Buffalo, NY. Email: pinaroku@buffalo.edu

<sup>5</sup>Cottingham Associate Professor, Glenn Dept. of Civil Engineering, Clemson Univ., Clemson, SC. Email: bross2@clemson.edu

<sup>6</sup>Associate Professor of Architecture, Structures, and Computation and Watt Family Innovation Center Faculty Fellow, School of Architecture, Clemson Univ., Clemson, SC.

Email: crbh@clemson.edu

## **ABSTRACT**

This paper introduces a new modular shear wall system designed for replaceability and resilience after extreme loading as well as architectural appeal. The walls are called tessellated structural-architectural (TeSA) walls because they consist of interlocking tiles (modules) with repetitive shapes (tessellations) and are intended to satisfy both structural and architectural demands. In TeSA systems, tile discontinuities may be able to contain damage within discrete units. This can facilitate quicker structural repair and reoccupation, and reduction of ensuing financial losses from service interruptions. Tiles of TeSA systems can be interlocking in one or two directions and can incorporate self-centering post-tensioning. This study focuses on documenting and quantifying damage in TeSA shear walls with tiles interlocking in one direction based on (1) laboratory tests performed on walls and (2) finite element modeling of TeSA walls. The considered TeSA walls consisted of reinforced concrete tiles and had selfcentering post-tensioning. The interlocking tiles did not need mechanical connections to adjacent tiles. Wall damage was quantified in terms of the number of damaged tiles as observed through testing and obtained through analyses. Finite element analyses of the TeSA shear wall were performed in open-source analysis software (OpenSees). Static pushover analyses were performed to obtain force-displacement relationship and ensuing damage. A framework for calculating probability of damage at salient drifts is presented considering uncertainties in tile-interface properties, modeling approach, and applied loading. The 1-D interlocking TeSA wall had a 9% probability of no damage and 91% probability of slight damage at the drift of 0.87%. The framework can be used to generate fragility functions for the TeSA wall.

**Keywords:** Resilience; Modular construction; Shear wall; Tessellated structural-architectural systems; Damage.

#### 1. INTRODUCTION

Modular construction is gaining popularity because of offsite prefabrication, quicker construction and better quality control. The behavior of modular structures depends on the type of connection between the modules [1]. Tessellated structural-architectural (TeSA) systems, comprising discrete interlocking tiles (modules), come under the purview of modular structures. They combine the advantages of modular structures with the architectural benefits of tessellations. When TeSA modules interlock, TeSA walls do not require connections between the modules. Such systems have acceptable performance as lateral load resisting systems [2, 3]. TeSA walls may help contain damage within individual tiles due to discontinuities, and reduce losses due to structural damage. Bao and Li [4] tested a prototype footbridge made of Engineered Cementitious Composites or bendable concrete [5], employing "Lego-inspired construction", and reported reasonable load-carrying capacity with acceptable deflections for dead and pedestrian loads. Javan et al. [6] tested an assembly plate made up of topologically interlocking concrete tessellations with rubber interfaces and reported substantially lower damage as compared to equivalent monolithic concrete plate. Meanwhile, only a few studies by the authors explored shear wall systems composed of topologically interlocking modules through analytical and experimental methods [2, 3, 7,8].

This study characterizes and quantifies damage in TeSA shear walls based on laboratory tests performed on walls with tiles interlocking in one direction [7], and finite element modeling thereof. The walls consisted of reinforced concrete tiles with no mechanical connections to adjacent tiles. The walls had self-centering post-tensioning. The damage experienced by the TeSA wall was quantified in terms of number of damaged tiles as observed through testing and obtained through analyses. Static pushover analyses of the TeSA shear wall were performed in an open-source analysis software (OpenSees) [10]. Probability of damage for a sample drift considering uncertainties in properties of tile interface, modeling approach, and applied loading, is calculated to give better insights into the performance of such systems.

# 2. DESCRIPTION OF THE TESA WALL AND TESTING

A TeSA wall with tiles interlocking in one direction (1-D interlocking) was designed and tested at Clemson University by Crocker et al. [7]. The specimen was 2896 mm (114 inches) high and 1854 mm (73 inches) long (aspect ratio of 1.56), with thickness of 140 mm (5.5 inches). The wall comprised four different shapes of tiles (I, C, T and L tiles) and had seven 15 mm (0.6 inch) diameter low-relaxation unbonded post-tensioning strands running though the center of the vertically-aligned tiles. The individual tiles did not have any mechanical connections to adjacent tiles. The representative layout of the specimen and different tiles are shown in Figure 1a and 1b respectively.

The individual tiles were made of reinforced concrete. The 28-day compressive strength of concrete was 47 MPa (6.8 ksi), and #3 Grade 60 rebars with a specified yield strength of 413 MPa (60 ksi) were used for reinforcement. The post-tensioning stands, with nominal strength of 1860 MPa (270 ksi), were stressed to approximately 696 MPa (101 ksi) or 97.8 kN (22 kips) force per strand for applying an axial load of 685 kN (154 kips) or 5.6% of the axial capacity of the wall. Spaces between tiles were filled with grout for better seating, ease of assembly, and removing potential gaps between the tiles. The grout did not have sufficient strength to carry shear and tensile stresses across tile-tile interfaces. More details about the design, fabrication, and testing of the specimen can be found in Crocker et al. [7].

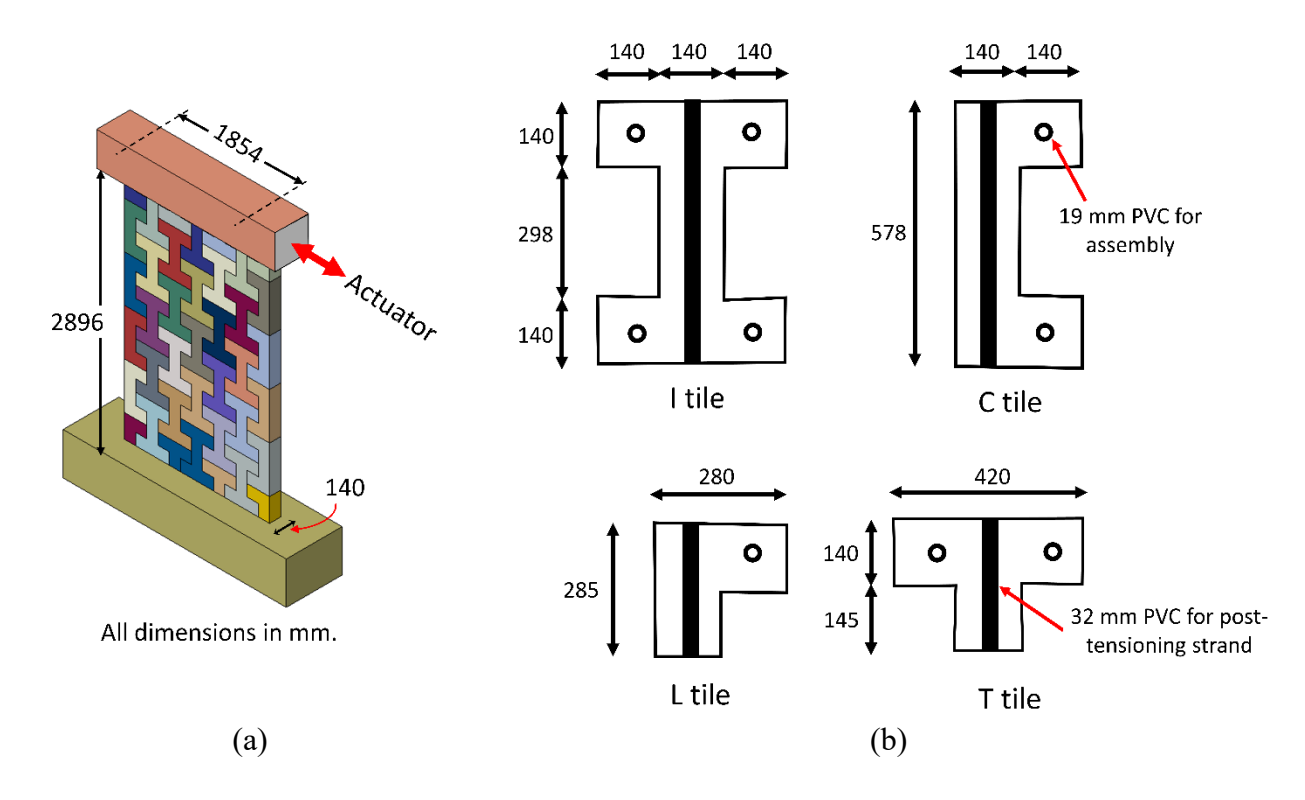


Figure 1. a) 1-D TeSA wall layout, b) tile shapes used in the wall.

The wall was subjected to eleven cycles of displacement at the top by means of an actuator and loading beam, with each cycle being repeated three times. The maximum drift that the wall was subjected to was 2.85% for the final cycle. The 1-D TeSA wall specimen is shown in Figure 2.



Figure 2. The 1-D TeSA wall specimen (image by author) [9].

#### 3. FINITE ELEMENT MODELING OF 1-D TESA WALL

A two-dimensional finite element (FE) model of the 1-D interlocking TeSA wall was built in OpenSees [10]. Each tile of the wall was modeled using displacement-based beam-column fiber elements (Figure 3). After analyzing the sensitivity of the results to the number of elements and number of integration points per element, the number of elements for I, C, T and L tiles was taken as 8, 6, 4, and 3 respectively, with the number of integration points per element being 3. The *Concrete02* model with linear tension softening from the OpenSees material model library was used to simulate concrete behavior. Bilinear *Steel02* (with yield strength of 413 MPa (60 ksi) and considering strain hardening) was used for modeling tile reinforcement. Post-tensioning strands were similarly modeled using bilinear *Steel02* with yield stress of 1674 MPa (243 ksi) and 1860 MPa (270 ksi) ultimate stress. An initial stress of 696 MPa (101 ksi) was directly applied to the strands for simulating post-tensioning and application of axial load. The tiles at the foundation were hinged at the base nodes, and the nodes at the top of the topmost tile layer were connected by an elastic steel beam.

For defining the inter-tile contact along the vertical and the horizontal directions, twoNodeLink elements were used. These links enable the transfer of forces across tile interfaces along both the horizontal and the vertical directions. Two types of links were defined: (a) vertical links and (b) horizontal links, based on the orientations thereof. The FE model, and the two types of links with their respective stiffness are shown in Figure 3.

For the vertical links, the axial behavior was modeled using compression only "Elastic-No Tension (ENT) material" to allow opening of gaps along tile interfaces. The compression stiffness in the axial direction was taken the same as that of grout that was placed between tiles of the test specimen. The tension stiffness in the axial direction and the rotational stiffness were zero. The lateral stiffness of the vertical links was based on friction between tiles. The lateral force resisted at any cross section of the wall was assumed to be distributed between the vertical links and tile webs crossing that section in proportion to contact/cross section areas thereof. All vertical links were assumed to resist equal lateral load and their lateral behavior (simulating friction) was defined using an "Elastic-Perfectly Plastic (EPP)" material. The elastic stiffness in the lateral direction was of the order of that of steel. The force at which the material becomes plastic in the lateral direction was assumed to be equal to the axial force per link multiplied by an assumed friction coefficient. The coefficient of friction was taken as 0.6 per ACI 318-14 [11]. The assumption of equal contribution of vertical links towards a part of frictional force generated at a section may not be accurate as any gaps opening on the tension side of the wall during lateral loading will disengage the friction. However, the frictional force will increase on the compression side due to increase in effective normal force, thereby offsetting the loss of friction experienced on the tension side. This notion is used to rationalize use of the average frictional force across all vertical links.

For the horizontal links, the compression stiffness in the axial direction was the stiffness of the grout that was placed between the tiles of the test specimen. The tension stiffness in the axial direction, the lateral stiffness and the rotational stiffness were zero.

# 4. STATIC PUSHOVER ANALYSIS AND MODEL VALIDATION

The FE model of the 1-D interlocking TeSA wall was subjected to a static push at the top with a peak drift of 2.85%. The pushover curve for the wall was obtained from the model and

compared with the backbone curve extracted from the cyclic test data. Figure 4 shows the force-displacement curve from the model and testing.

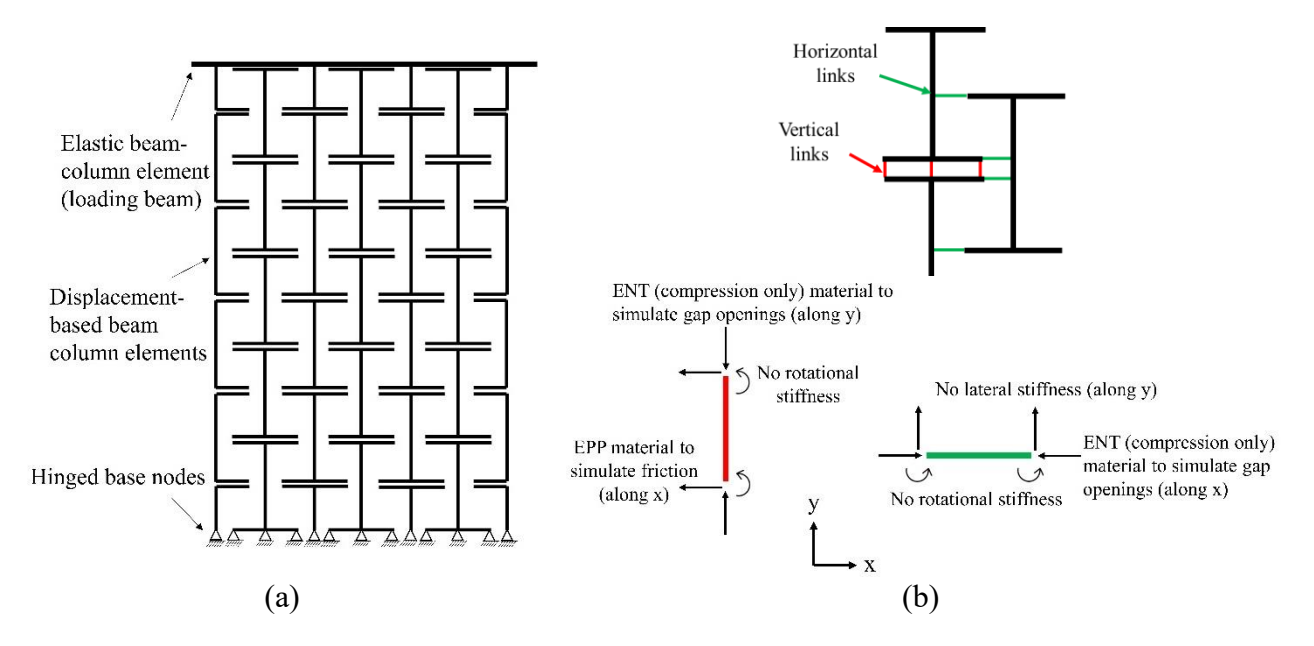


Figure 3. a) Two dimensional model of the 1-D TeSA wall (links not shown for clarity), b) Vertical and horizontal *twoNodeLink* elements used for inter-tile contact definition.

The model captures the peak strength reasonably well with an exact match of peak force at 1.75% drift. The strength mismatch (20% error) at ultimate drift of 2.85% was due to yielding of connections between the foundation and base tiles observed in the test specimen but not captured by the FE model. The FE model also predicts a slightly stiffer wall, because: (1) the backbone curve is extracted from cyclic force-displacement data, and (2) foundation flexibility is not accounted for by the FE model.

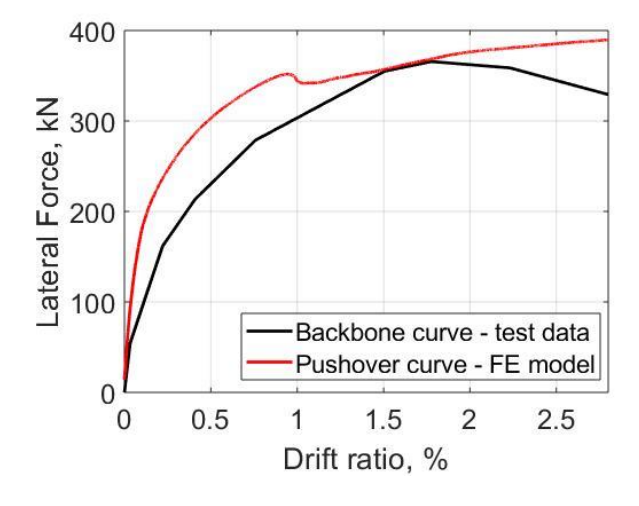


Figure 4. Comparison of backbone (test-data) and pushover (FEA) curves for 1-D TeSA wall.

The FE model captures the force-displacement behavior reasonably well and is hence validated.

# 5. DAMAGE EVALUATION OF THE 1-D INTERLOCKING TESA WALL

The tiles of the 1-D TeSA wall specimen were evaluated for damage based on crack widths and extent of spalling of concrete using recommendations from FEMA 306 [12], FEMA 58-1/BD-3.8.8 [13] and FEMA 58-1/BD-3.8.9 [14]. Each tile was classified under four damage categories: undamaged, slight, moderate, and severe. For the FE model, the maximum compressive and tensile strains in a tile were used to define damage states of each tile. Compressive and tensile strain thresholds that correspond to each damage state were calibrated by matching the number of tiles for each damage state from the analyses with those observed during testing at salient drifts. The final strain thresholds and criteria for damage are summarized in Table 1.

	Test	FE model			
Damage state	Crack width/ concrete spalling	Tensile strain (ε <sub>ι</sub> ) range	Compressive strain (ε <sub>c</sub> ) range		
No damage	_	$\varepsilon_{t} \leq 0.00300$	$\varepsilon_{\rm c} <= 0.00127$		
Slight	Crack width <3 mm	$0.00300 \le \epsilon_{\rm t} \le 0.01270$	$0.00127 \le \varepsilon_{\rm c} \le 0.00220$		
Moderate	<ol> <li>Crack width ≥3 mm</li> <li>Minor spalling</li> </ol>	$0.01270 \le \epsilon_{\rm t} < 0.07000$	$0.00220 \le \epsilon_{c} < 0.03200$		
Severe	Major spalling (>51 mm sized chunks at toes)	$\epsilon_{t} >= 0.07000$	$\varepsilon_{c} >= 0.03200$		

Table 1. Damage criteria used during testing and in FE analysis.

The final damage distribution predicted by the FE model per the aforementioned criteria for a sample cycle (cycle 9), with maximum drift of 1.85%, is shown in Figure 5. During testing, 22 tiles out of a total of 39 tiles were reported to be damaged (15 tiles slightly and 7 tiles moderately damaged). Since the FE analyses were pushover, not cyclic, all tiles placed symmetrically about the center of the wall were assigned the same damage state in the analyses when comparing the analysis and cyclic test results. FE model predicted a total of 26 tiles damaged (13 tiles slightly and 13 tiles moderately damaged), which was deemed reasonably close to the test observation.

## 6. PROBABILITY OF DAMAGE

The probability of damage for a sample drift of the wall was evaluated considering uncertainties in applied loading, modeling approach and tile-interface properties (coefficient of friction). The applied load consists of permanent load (G) and imposed load (Q) defined for a specified renewal period (5 years herein). The former follows lognormal distribution and the latter follows Gumbel distribution [15]. Model uncertainty was assumed to follow lognormal distribution [15, 16]. For simplicity, the model uncertainty and the uncertainty in applied load were combined into a single lognormal random variable, P.

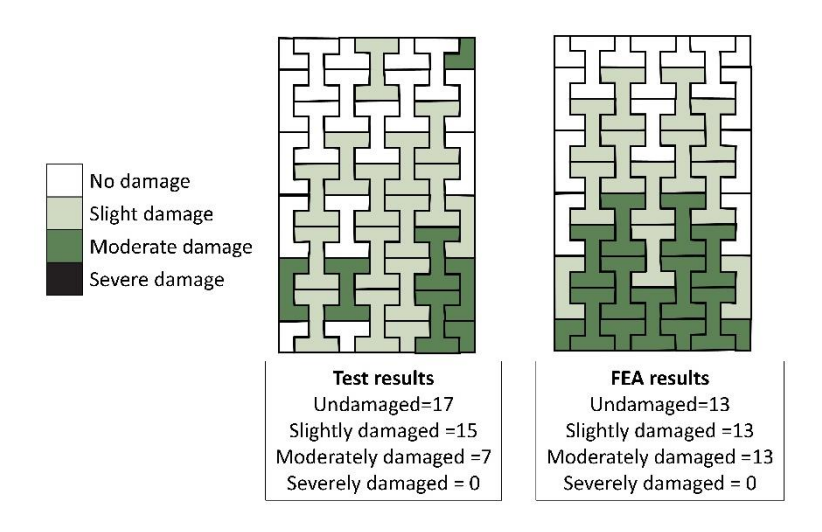


Figure 5. Damage distribution for 1-D TeSA wall as reported at the end of cycle 9 of testing and as predicted by the FE model.

A value of coefficient of friction was used to characterize the lateral stiffness of vertical links to simulate friction (as discussed in section 3). The coefficient of friction value ( $\mu$ ) considered for calculating the cap on peak friction force per vertical link was taken as 0.6, which is the lower-bound value for smooth joint condition (cold joint) between two concrete layers per ACI 318-14 [11]. Krc et al. [17] created a database for shear friction tests conducted over the past few decades for different concrete interface conditions. The data provided for cold-joint interface conditions were processed to evaluate the mean and standard deviation. Coefficient of friction can be reasonably assumed to follow lognormal distribution [18]. The statistical parameters for the two random variables P and  $\mu$  to be considered herein are summarized in Table 2.

Table 2. Statistical parameters of the two considered random variables

Random variable	Applied load (P), kN	Coefficient of friction (µ)			
Mean	467.10	0.68			
Standard deviation	91.20	0.15			
Coefficient of variation	0.20	0.22			

For each random variable, 10 random realizations were generated using Latin Hypercube sampling (LHS). LHS can be used for efficient sampling when lower number of realizations are needed for computational economy [19]. The random realization for the two random variables under discussion, generated using LHS, are shown in Table 3.

For the current study, 100 simulations were run and the probabilities of attaining a damage state were reported for a sample wall drift of 0.87% (displacement of 1 inch). The four damage states described earlier were used. The TeSA wall was attributed the damage state that the majority of tiles of the wall attained for a simulation. For example, a TeSA wall was assumed to have severe damage at a drift if the majority of tiles had severe damage at that drift. At 0.87% drift, 9, 91, 0 and 0 simulations out of a total of 100 simulations resulted in no, slight, moderate and severe damage in the 1-D interlocking TeSA wall, respectively. The probabilities of a damage state being attained for the sample drift are shown in Figure 6.

Random variable	Random realizations									
	1	2	3	4	5	6	7	8	9	10
Coefficient of friction	0.48	0.54	0.57	0.59	0.63	0.68	0.71	0.77	0.80	0.90
Applied load, kN	352.33	374.52	401.08	426.16	449.03	478.12	489.68	533.36	568.14	613.07

Table 3. Random realizations of random variables

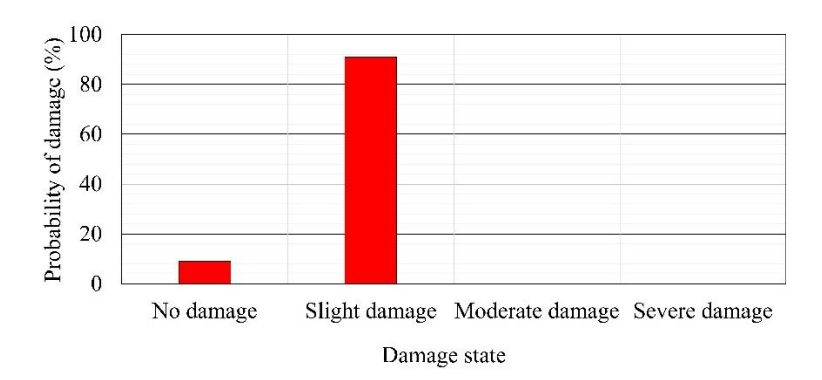


Figure 6. Probabilities of attaining different damage states for sample drift of 0.87%.

#### 7. SUMMARY AND CONCLUSIONS

The current study developed a streamlined finite element model of tessellated structural-architectural shear walls topologically interlocking in one direction (1-D interlocking TeSA walls) to evaluate damage while incorporating uncertainties in the input parameters. The FE model was validated with test data. It captured the global force-displacement behavior of the wall and damage distribution with reasonable accuracy. It predicted the peak strength observed in testing well but mismatched the peak strength at ultimate drift by approximately 20%. This was due to the inability of the FE model to capture the yielding of anchor bolts connecting the base tiles to the foundation. The slight mismatch for initial stiffness was due to the flexible foundation not being incorporated in the FE model.

For characterizing the state of damage in a tile during testing, damage criteria – informed by existing literature - were created based on crack size and level of spalling. Using the validated analyses, damage states of tiles were defined according to the maximum compressive and tensile strains in each tile. For each damage state, compressive and tensile strain ranges were defined. These strain ranges were calibrated to match the number of tiles per damage state obtained from the analyses and testing at salient drifts. For example, the FE model predicted a total of 26 damaged tiles (13 slightly and 13 moderately damaged) at a drift of 1.85%, whereas 22 tiles were reported damaged (15 slightly and 7 moderately damaged) during testing. The state of damage of the wall was then defined as the damage state that the majority of tiles attained for a particular drift.

A framework for calculating the probability of a damage state being attained for the wall was proposed considering variations in the applied axial load and the coefficient of friction between tiles. Uncertainty arising from the modeling approach was combined with that of the applied axial load. Ten random realizations of the two aforementioned random variables were generated

using Latin Hypercube sampling technique and 100 simulations were run for a sample wall drift of 0.87%. The simulations that resulted in no wall damage were 9 in number and those resulting in slight damage were 91, with no simulation resulting in moderate or severe wall damage.

## ACKNOWLEDGEMENTS

This material is based upon work supported by the National Science Foundation under Grant Nos. 1762133 and 1762899. Any opinions, findings, and conclusions or recommendations expressed in this material are those of the authors and do not necessarily reflect the views of the National Science Foundation. Clemson students Mikayla Baker and Seth Moore assisted in mapping damage in the tested shear wall.

## REFERENCES

- [1] A. W. Lacey, W. Chen, H. Hao, and K. Bi. (2018). Structural response of modular buildings an overview. *Journal of Building Engineering*. 16:45-56.
- [2] B. E. Ross, C. Yang, M. C. B. Kleiss, P. Okumus, and N. Elhami-Khorasani. (2020). Tessellated structural-architectural systems: Concept for efficient construction, repair, and disassembly. *Journal of Architectural Engineering*. 26:04020020.
- [3] M. Syed, M. Moeini, P. Okumus, N. Elhami-Khorasani, B. E. Ross, and M. C. B. Kleiss. (2021). Analytical study of tessellated structural-architectural reinforced concrete shear walls. *Engineering Structures*. 244:112768.
- [4] Y. Bao, and V. C. Li. (2020). Feasibility study of lego-inspired construction with bendable concrete. *Automation in Construction*. 113:103161.
- [5] V. C. Li. (2019). High-performance and multifunctional cement-based composite material. *Engineering*. 5:250-60.
- [6] A. R. Javan, H. Seifi, X. Lin, and Y. M. Xie. (2020). Mechanical behaviour of composite structures made of topologically interlocking concrete bricks with soft interfaces. *Materials & Design*. 186:108347.
- [7] G. F. Crocker, B. Ross, M. Kleiss, P. Okumus, N. Elhami-Khorasani, and J. Romero. (2021). Fabrication and erection of precast concrete tessellated walls: practical considerations. *Precast/Prestressed Concrete Institute National Convention*.
- [8] M. E. Abdelmoneim Elsayed, G. F. Crocker, B. E. Ross, P. Okumus, M. C. Kleiss, and N. Elhami-Khorasani. (2021). Finite element modeling of tessellated beams. Journal of Building Engineering.103586.
- [9] G. F. Crocker. (2021). Personal communication.
- [10] F. McKenna, G. Feneves, and M. Scott. (2000). *Open system for earthquake engineering simulation (OpenSees)*. University of California, Berkeley, CA.
- [11] ACI. (2014). Building code requirements for structural concrete (ACI 318-14) and commentary (ACI 318 R-14). Farmington Hills, MI. American Concrete Institute.
- [12] FEMA. (1998). Evaluation of earthquake damaged concrete and masonry buildings basic procedures manual (FEMA 306). Washington, DC. Federal Emergency Management Agency.
- [13] FEMA. (2009). Damage states and fragility curves for low aspect ratio reinforced concrete walls (FEMA 58-1/BD-3.8.8). Washington, DC. Federal Emergency Management Agency.

- [14] FEMA. (2011). Fragility functions for slender reinforced concrete walls (FEMA 58-1/BD-3.8.9). Washington, DC. Federal Emergency Management Agency.
- [15] M. Holický, and M. Sýkora. (2010). Stochastic models in analysis of structural reliability. *Proceedings of the international symposium on stochastic models in reliability engineering, life sciences and operation management.* Beer Sheva, Israel.
- [16] JCSS. (2001). *JCSS Probabilistic Model Code*. Zurich, Switzerland: Joint Committee on Structural Safety.
- [17] K. Krc, S. Wermager, L. H. Sneed, and D. Meinheit. (2016). Examination of the effective coefficient of friction for shear friction design. *PCI Journal*. 61.
- [18] C. Steele. (2008): Use of the lognormal distribution for the coefficients of friction and wear. *Reliability Engineering & System Safety*. 93:1574-6.
- [19] A. Olsson, G. Sandberg, and O. Dahlblom. (2003). On Latin hypercube sampling for structural reliability analysis. *Structural safety*. 25:47-68.